IEEE Photonics Journal
An IEEE Photonics Society Publication

Fiber-Optic Curvature Sensor Based on Cladding-Mode Bragg Grating Excited by Fiber Multimode Interferometer

Volume 4, Number 3, June 2012

Wenjun Zhou
Yan Zhou
Xinyong Dong, Member, IEEE
Li-Yang Shao
Jia Cheng
Jacques Albert, Member, IEEE

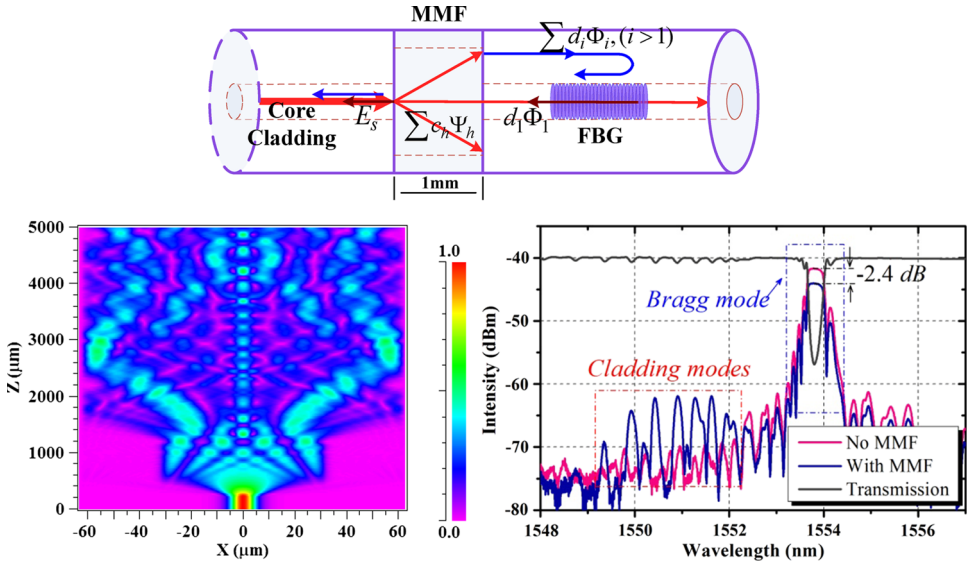

DOI: 10.1109/JPHOT.2012.2202895
1943-0655/$31.00 ©2012 IEEE

IEEE photonics SOCIETY

IEEE

Fiber-Optic Curvature Sensor Based on Cladding-Mode Bragg Grating Excited by Fiber Multimode Interferometer

Wenjun Zhou,[1,2] Yan Zhou,[1,3] Xinyong Dong,[1] *Member, IEEE*, Li-Yang Shao,[1] Jia Cheng,[3] and Jacques Albert,[2] *Member, IEEE*

[1]Institute of Optoelectronic Technology, China Jiliang University, Hangzhou 310018, China
[2]Department of Electronics, Carleton University, Ottawa, Ontario K1S 5B6, Canada
[3]Zhejiang Province Institute of Metrology, Hangzhou 310013, China

DOI: 10.1109/JPHOT.2012.2202895

Manuscript received April 20, 2012; revised May 28, 2012; accepted May 29, 2012. Date of publication June 8, 2012; date of current version June 19, 2012. This work was supported by the National Basic Research Program of China (973 Program) under Grant No. 2010CB327804, the National Natural Science Foundation of China under Grant No. 61007050, Qianjiang Talent Project in Zhejiang province of China under Grant No. QJD1002002, project supported by the National Science and Technology support funded of China under Grant No. 2011BAF06B02, project funded by Shanghai Science and Technology commission of China under Grant No. 10595812300. J. Albert acknowledges the support of the Canada Research Chairs program and the Natural Sciences and Engineering Research Council of Canada. Corresponding author: X. Dong (e-mail: xydong@cjlu.edu.cn).

Abstract: A sensing structure consisting of a short multimode fiber (MMF) spliced in just upstream of a uniform fiber Bragg grating (FBG) is proposed and experimentally demonstrated for temperature-independent curvature measurement. The short MMF section generates cladding modes in the fiber that contains the FBG. Several of these modes get reflected back by the FBG at shorter wavelengths and re-enter the launch fiber after passing through the MMF section. The net recoupling efficiency between the incident forward core mode and reflected cladding modes is -20 dB when the fiber is straight, but decays when a curvature applied on the sensing structure. A maximum sensitivity of 0.74 dB/m^{-1} is obtained in a large measurement range up to $\sim$15.5 m^{-1}, with no orientation dependence of the sensitivity. The reflected coupled power variation is measured to be $\pm$0.15 dB over the temperature range from 0 to 70 °C, allowing for temperature-independent curvature measurements.

Index Terms: Fiber Bragg grating, multimode fiber, curvature measurement, temperature-independent.

1. Introduction

Curvature measurement is significant in various applications, ranging from security monitoring to structural engineering. Fiber-optic sensors offer a great number of advantages over conventional sensors, such as electrically passive operation, immunity to electromagnetic interference, high sensitivity, integrated structure, and potentially low cost. In recent years, fiber gratings have been widely investigated and applied in curvature measurement. For example, long-period gratings (LPGs) possess a high sensitivity in curvature-induced wavelength shift and amplitude change of the transmission resonances. But they also show a high temperature cross-sensitivity and a wide bandwidth of the transmission resonances that leads to reading errors and difficulty in multiplexing [1]–[3]. Alternatively, chirped fiber Bragg gratings (CFBGs) can be used for curvature measurement by relating the chirp rate (i.e., reflection bandwidth) to the bending of a substantially flexible beam

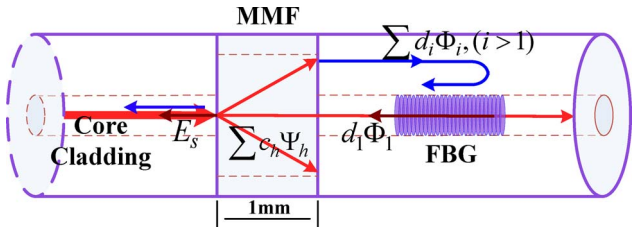

Fig. 1. Schematic diagram of the cladding modes excitation and recoupling mechanisms in the proposed sensing structure.

[4], [5]. However, the mechanically bulky beam-based fiber grating sensors become inflexible and awkward in some microscale environmental measurements. Finally, tilted fiber Bragg gratings (TFBGs) are also sensitive to curvature because the coupling coefficients of cladding modes (low-order cladding modes in particular) change as the fiber is bent [6]. The drawbacks of this configuration are that transmission measurements are required and that the number of low order nearly degenerate cladding modes involved is large. As a result, the net transmission spectrum changes irregularly with curvature and shows strong orientation dependence.

In order to overcome some of the difficulties in quantifying curvature from the transmission spectra of TFBG, configurations involving the recoupling of backward propagating cladding modes into a reflected core mode were reported. Guo proposed a core-offset splicing structure located a short distance upstream of the TFBG for recoupling the bend sensitive backward cladding modes [7] and also for external refractive index measurements [8]. Moreover, this kind of configuration allows for real time measurements of the cladding mode power reflected using bandpass filtering and a photodiode. Other in-line fiber structures were also proposed for recoupling the backward propagating cladding modes of TFBG, such as a biconical taper [9], [10], multimode fiber (MMF) [11], and LPG [12], which were also effective in curvature measurement. For the aforementioned TFBG-based curvature sensors, the sensitivity depends on the orientation of the bending direction relative to the tilt plane of the TFBG, which allows for the simultaneous measurement of the magnitude and direction of the bend. On the other hand, this directional sensitivity requires additional calibration in practical applications and complicates the sensor demodulation. As a cylindrically symmetrical structure, a FBG has no intrinsic directional sensitivity change under bending but can be used as a sensor when coupled with an upstream core-offset splicing point [13]. However, the core-offset splicing point used in [13] breaks the cylindrical symmetry and reintroduces a bend orientation sensitivity.

In this paper, an orientation-insensitive curvature sensor based on the reflection of cladding modes from a core-inscribed FBG is proposed and experimentally demonstrated. A short section of MMF was inserted upstream of the FBG and serves as a cylindrically symmetric core-cladding modal coupler to excite cladding modes into the fiber that contains the FBG and to recapture reflected cladding modes back into the core of the launch fiber. The recaptured cladding modes appear on the short wavelength side of the Bragg (core mode) resonance because their effective index is lower. The efficiency of the back reflection is much lower (-20 dB) for the cladding modes because of their relatively poor overlap with the refractive index modulation located in the core of the fiber. It must be emphasized that unlike the case of the TFBG, the cladding modes are individually reflected upon themselves by the FBG, and do not appear due to coupling from a core mode. When a curvature is applied on the sensing structure, the intensity of the recaptured cladding modes decays significantly and monotonically, independently of the direction of the bend. Finally, the performance of the sensor is shown experimentally to be independent of the temperature of operation.

2. Operation Principle and Sensor Fabrication

Fig. 1 shows the schematic diagram of the proposed sensing structure, containing a section of MMF with a length of 1 mm and a uniform FBG. The MMF is inserted at a location upstream from the FBG. The single mode of the injected light propagating in the lead-in single-mode fiber (SMF)

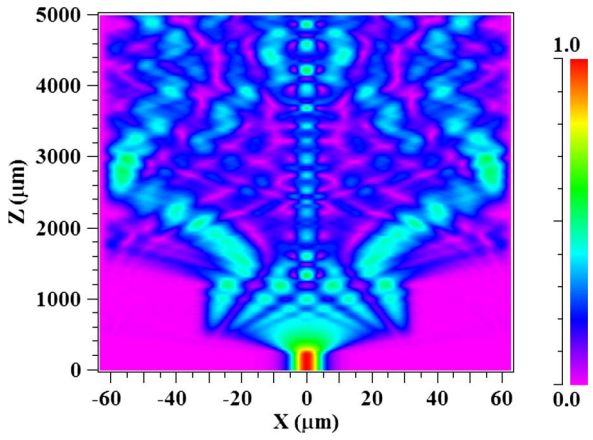

Fig. 2. BPM simulation of the light propagation along the SMF–MMF–SMF structure.

excites multiple modes of the MMF due to the modal mismatch. These modes then propagate and interfere in the MMF section up to the end, where they further excite both core and cladding modes of the SMF which contains the FBG. The coupling coefficient of the *i*th order mode d_i in the lead-out SMF can be expressed as [14], [15]

$$d_i = \frac{\int_0^{2\pi}\int_0^{\infty}\sum_{h=1}^{M} c_h \Psi_h(r,\theta)\exp(j\beta_h z) \times \Phi_i(r,\theta)^* r\, dr\, d\theta}{\int_0^{2\pi}\int_0^{\infty} |\Phi_i(r,\theta)|^2 r\, dr\, d\theta} \tag{1}$$

where c_h is the excitation coefficient, Ψ_h is the field profile, β_h is the propagation constant, of the *h*th eigenmode in the MMF, respectively, and *M* is the total number of guided modes inside the MMF; Φ_i is the *i*th mode in lead-out SMF, consisting of core mode $(i = 1)$ and cladding modes $(i > 1)$. The excitation coefficients c_h in the MMF can be calculated from the following cross-correlation formula similar with (1)

$$c_h = \frac{\int_0^{2\pi}\int_0^{\infty} E_s(r,\theta) \times \Psi_h(r,\theta)^* r\, dr\, d\theta}{\int_0^{2\pi}\int_0^{\infty} |\Psi_h(r,\theta)|^2 r\, dr\, d\theta} \tag{2}$$

where E_s is the field distribution of the fundamental mode in SMF. It is obvious that the coefficient d_i is determined by parameters of MMF, such as core diameter, refractive index and length of the inserted MMF. As the SMF–MMF–SMF structure is bent, the field patterns of the MMF modes will be altered, leading to changes in the c_h coefficients. The bending also changes their propagation constants, thereby changing the multimode interference pattern at the output of the MMF section and hence the amplitudes of the individual excitation coefficients d_i. These effects are magnified by the double passage of light reflected from the FBG in the MMF.

Fig. 2 shows the simulated amplitude distribution of the light propagating along the MMF (200–1200 μm in Z axis) by using the propagation beam method (BPM), demonstrating that the injected light spreads significantly in the MMF section and couples strongly into cladding modes of the lead-out SMF as mentioned above. The parameters of the MMF used in our simulation are set as follows: core diameter of 62.5 μm, core refractive index of 1.4662, cladding refractive index of 1.45, and length of 1 mm. A similar multimode interference effect occurs in the cladding of the lead out fiber but each cladding mode is individually reflected from the FBG (not shown in the unidirectional BMP model we used) and the coupling mechanisms are reversed in the return trip, finally leading to some recapture of reflected cladding modes by the SMF lead-in fiber.

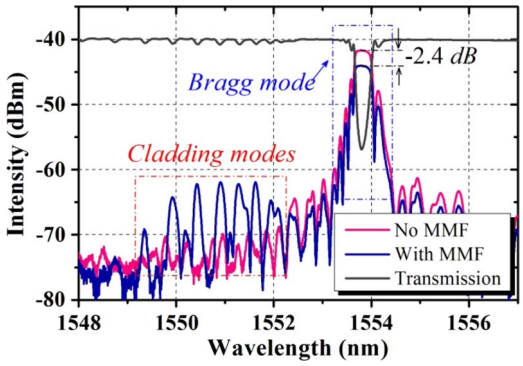

Fig. 3. Transmission spectrum of the original FBG and spectral comparison of the reflection spectra before and after inserting the MMF.

A uniform FBG was written in a hydrogen-loaded photosensitive SMF with a scanning 244 nm UV laser beam using the phase-mask method. The achieved FBG has a reflectivity of 98%, a length of 8 mm, a center Bragg wavelength of 1553.78 nm (at room temperature), and a 3-dB spectral bandwidth of 0.34 nm. The transmission spectrum of the inscribed FBG is shown in Fig. 3, where some weak cladding-mode resonances appear on the short wavelength side of the Bragg resonance. It is important to note that these weak dips arise from the coupling of core mode light to cladding modes, as there are no incident cladding modes on the FBG prior to splicing the MMF. They are also much smaller than the strong cladding-mode resonances caused by tilt planes in a TFBG. In order to splice a short section of MMF, we cleaved the SMF 5 mm upstream from the FBG, and spliced it with a long section of step-index MMF (with a core diameter of 62.5 μm), then cleaved the MMF 1 mm back of the original splicing point and finally splicing this structure to a SMF. The reason for the short separation between the MMF and the FBG is that the excited modes propagating in the cladding suffer large losses. The reflection spectrum of the fabricated sensing structure is shown in Fig. 3 and compared with the original spectrum of the FBG in the SMF alone. It can be seen that several reflected peaks appear in the wavelength range from 1549.2 to 1552.2 nm on the short side of Bragg peak after inserting the MMF. The amplitude of these emerging cladding modes is much smaller than that of reported hybrid structure composed of MMF and TFBG [11], [16], because the reflection efficiency of the FBG is much smaller for cladding modes than for the core mode (and also much smaller than the coupling of core modes to cladding modes by a TFBG). On the other hand, the intensity of Bragg mode reflection decreases by 2.4 dB due to the insertion loss of the MMF, which is about 3.33 times lower than that reported in [11]. The smaller loss is attributed to the shorter length of the inserted MMF (relative to 2 mm in [11]) and better splicing which improves the overall coupling coefficients of the core mode c_1 and d_1. The amplitudes of the reflected cladding modes can be also optimized by adjusting the length of MMF through the multimode interference effect. Based on previous works about SMF–MMF–SMF structures [17], increasing the length of the MMF section will increase the spectral modulation of the transmitted light and deteriorate the regularity of the spectral changes arising from bending. Moreover, the influence of temperature on the multimode interference pattern (and hence on the sensor response) decreases with decreasing length of MMF [18]. Compared with the previously reported curvature sensor composed of long MMF (32 mm) and LPG [19], the spectral modulation and temperature perturbation induced by the short MMF (1 mm) of this proposed sensor would be much smaller. Therefore, we spliced a short MMF section of only 1 mm to introduce the necessary modal mismatch for the excitation and recoupling of the cladding modes of the FBG.

3. Experimental Results and Discussion

Fig. 3 illustrates the experimental setup of the curvature measurement system. The light provided by a broadband light source (BBS) with flat output within the range from 1520 to 1620 nm goes

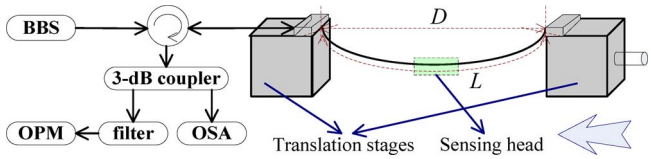

Fig. 4. Schematic diagram of the curvature measurement system.

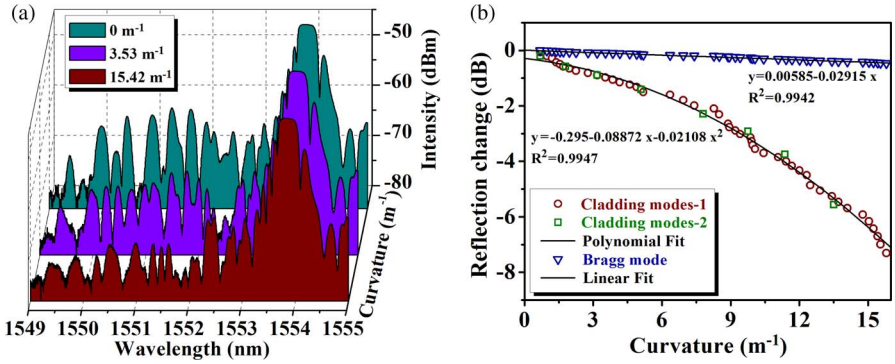

Fig. 5. (a) Reflection spectra of the FBG under different applied curvatures. (b) Amplitude change of the Bragg mode and cladding modes versus curvature. Cladding modes-1 and -2 are the responses of two curvature measurements under different bend directions.

through an optical circulator (OC) and is launched into the sensing structure. Then the light reflected by the FBG propagates through a 3-dB coupler that splits the reflected power into an optical spectrum analyzer (OSA) with a wavelength resolution of 0.01 nm and an optical power meter (OPM), respectively. A bandpass filter connected before the OPM is used to realize individual power measurement of the Bragg mode and of the cladding modes. The sensor response to curvature was examined by mounting the two ends of the sensing head on two translation stages and moving one stage inward to change the separation between them. The shape of the FBG located in the middle of the two stages is normally approximated as an arc circle. The curvature applied on the sensing structure can be calculated by the corresponding separation of the two stages, expressed as

$$\sin(LC/2) = DC/2 \tag{3}$$

where L is the length of fiber between the two mounted points, C is the applied curvature, and D is the separation of the two stages, which are marked in Fig. 4.

Fig. 5(a) shows the evolution of the reflection spectra under an increase of applied curvature. It is obvious that the amplitude of the cladding modes diminishes significantly with the increasing applied curvature, indicating that the bending of the sensing structure decreases the excitation and/or recoupling efficiency of the cladding modes. On the other hand, the core mode (Bragg mode) suffers much smaller changes because the core of the fiber lies on the neutral axis for pure bending and the core mode is relatively insensitive to the limited curvature. Besides, the number of reflected cladding modes under different curvatures also changes, demonstrating that new cladding modes with different orders are excited in the bent sensing structure. The relative changes of the reflected power of the cladding modes and core mode against the applied curvature are depicted in Fig. 5(b). Both the cladding modes and the core mode decay with the applied curvature monotonically. The response of the cladding modes measured in a fixed bending direction (red circle) shows that the sensitivity becomes higher with the increase of curvature, reaching a highest sensitivity of 0.74 dB/m^{-1} in the measurement range from 0 to 15.5 m^{-1}. Thus, the corresponding resolution of the curvature measurement can be obtained in 0.014 m^{-1}, based on the OPM's accuracy of 0.01 dB (assuming a

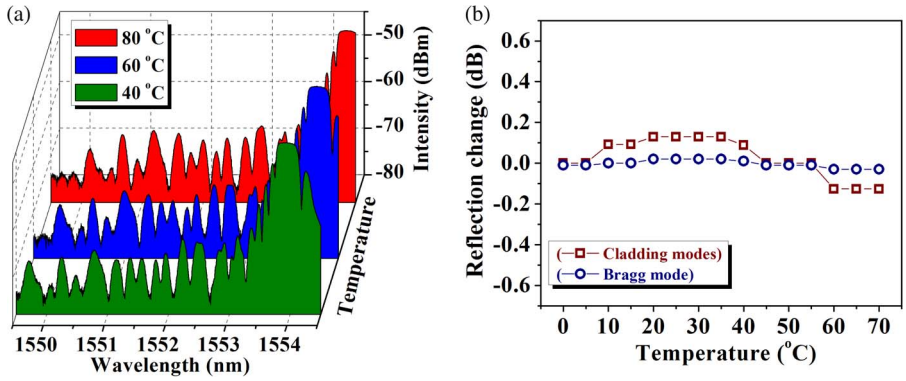

Fig. 6. (a) Reflection spectra of FBG under the different applied temperature. (b) Amplitude change of Bragg mode and cladding modes versus temperature.

sufficiently powerful light source so that the amplitude noise can be neglected). The curvature measurement in a different direction was also carried out, of which the response of the cladding modes is shown as the green squares in Fig. 5(b). There is no observable difference between the bending sensitivity in the two directions, meaning that the sensor is directionally independent. Meanwhile, the response of the Bragg mode shows a very small linear curvature sensitivity of 0.03 dB/m^{-1}, as expected, and a relative power measurement (using a 3 dB splitter and bandpass filters) between the cladding modes and the Bragg mode could be used to further eliminate noise and power fluctuations from the measurement.

The temperature response of the proposed sensing structure is also investigated by placing the unstrained sensor (with a small curvature) into an oven. Fig. 6(a) shows the red shift of the reflection spectra as the temperature increases, without significant amplitudes changes. The temperature-induced wavelength shifts of the core mode and cladding modes are almost equal due to the similar effective refractive indices. Quantitative measurements of the reflected power of the two kinds of modes versus the temperature are shown in Fig. 6(b). It can be seen that both the cladding modes and the Bragg mode have similar small variations in amplitude during the complete temperature measurement. However, the magnitude of the amplitude fluctuation of the cladding modes ($\sim\pm$0.15 dB) is much larger than that of the Bragg mode (0.03 dB). This difference may be due to the much larger bend sensitivity of the cladding modes to bending and the possibility that the grating moved slightly during the experiment (due to the internal fan of the oven). This residual temperature dependence could be further reduced by making sure that the sensor package does not bend as a result of temperature change and also by careful optimization of the MMF section parameters. If the temperature effect of the cladding mode can be reduced to the same level as that of the Bragg mode, the highest temperature-induced error would be $\sim$0.04 m^{-1}. Therefore, the proposed sensing structure can achieve temperature-independent and orientation-independent curvature measurements.

4. Conclusion

A temperature-independent curvature sensor formed by splicing a short section of MMF to a FBG is proposed in this work. The modal mismatch between MMF and SMF causes the excitation and recoupling of the cladding modes of the FBG, and these coupling mechanisms are sensitive to the applied curvature. The experimental performance demonstrated that the proposed sensor has a consistent sensitivity in all bending directions due to the symmetrical structure, which is a significant advantage over TFBG and other noncylindrically symmetrical sensors in applications where orientation information is not needed. The optimization of the reflected cladding modes spectral and power characteristics, and of the temperature sensitivity, will be carried out by more exhaustive studies of the MMF section design in our future work.

References

[1] L.-Y. Shao, J. Zhao, X. Dong, H. Y. Tam, C. Lu, and S. He, "Long-period grating fabricated by periodically tapering standard single-mode fiber," *Appl. Opt.*, vol. 47, no. 10, pp. 1549–1552, Apr. 2008.

[2] T. Allsop, K. Kalli, K. Zhou, Y. Lai, G. Smith, M. Dubov, D. J. Webb, and I. Bennion, "Long period gratings written into a photonic crystal fiber by a femtosecond laser as directional bend sensors," *Opt. Commun.*, vol. 281, no. 20, pp. 5092–5096, Oct. 2008.

[3] Y. Liu, L. Zhang, J. A. R. Williams, and I. Bennion, "Optical bend sensor based on measurement of resonance mode splitting of long-period fiber grating," *IEEE Photon. Technol. Lett.*, vol. 12, no. 5, pp. 531–533, May 2000.

[4] X. Dong, H. Meng, Z. Liu, G. Kai, and X. Dong, "Bend measurement with chirp of fiber Bragg grating," *Smart Mater. Struct.*, vol. 10, no. 5, pp. 1111–1113, Oct. 2001.

[5] W. Zhou, X. Dong, K. Ni, C. C. Chan, and P. Shum, "Temperature-insensitive accelerometer based on a strain-chirped FBG," *Sens. Actuators A, Phys.*, vol. 157, no. 1, pp. 15–18, Jan. 2010.

[6] S. Baek, Y. Jeong, and B. Lee, "Characteristics of short-period blazed fiber Bragg grating for use as macro-bending sensors," *Appl. Opt.*, vol. 41, no. 4, pp. 631–636, Feb. 2002.

[7] T. Guo, A. Ivanov, C. Chen, and J. Albert, "Temperature-independent tilted fiber Bragg grating vibration sensor based on cladding-core recoupling," *Opt. Lett.*, vol. 33, no. 9, pp. 1104–1106, May 2008.

[8] T. Guo, H. Y. Tam, P. A. Krug, and J. Albert, "Reflective tilted fiber Bragg grating refractometer based on strong cladding to core recoupling," *Opt. Exp.*, vol. 17, no. 7, pp. 5736–5742, Mar. 2009.

[9] T. Guo, L.-Y. Shao, H. Y. Tam, P. A. Krug, and J. Albert, "Tilted fiber grating accelerometer incorporating an abrupt biconical taper for cladding to core recoupling," *Opt. Exp.*, vol. 17, no. 23, pp. 20 651–20 660, Nov. 2009.

[10] L.-Y. Shao and J. Albert, "Compact fiber-optic vector inclinometer," *Opt. Lett.*, vol. 35, no. 7, pp. 1034–1036, Apr. 2010.

[11] Y. X. Jin, C. C. Chan, X. Y. Dong, and Y. F. Zhang, "Temperature-independent bending sensor with tilted fiber Bragg grating interacting with multimode fiber," *Opt. Commun.*, vol. 282, no. 19, pp. 3905–3907, Oct. 2009.

[12] L.-Y. Shao, A. Laronche, M. Smietana, P. Mikulic, W. J. Bock, and J. Albert, "Highly sensitive bend sensor with hybrid long-period and tilted fiber Bragg grating," *Opt. Commun.*, vol. 283, no. 13, pp. 2690–2694, Jul. 2010.

[13] C. Gouveia, P. A. S. Jorge, J. M. Baptista, and O. Frazão, "Temperature-independent curvature sensor using FBG cladding modes based on a core misalignment splice," *IEEE Photon. Technol. Lett.*, vol. 23, no. 12, pp. 804–806, Jun. 2011.

[14] W. Mohammed, P. Smith, and X. Gu, "All-fiber multimode interferometer bandpass filter," *Opt. Lett.*, vol. 31, no. 17, pp. 2547–2549, Sep. 2006.

[15] Q. Wu, Y. Semenova, B. Yan, Y. Ma, P. Wang, C. Yu, and G. Farrell, "Fiber refractometer based on a fiber Bragg grating and single-mode–multimode–single-mode fiber structure," *Opt. Lett.*, vol. 36, no. 12, pp. 2197–2199, Jun. 2011.

[16] B. Zhou, A. P. Zhang, S. He, and B. Gu, "Cladding-mode-recoupling-based tilted fiber Bragg grating sensor with a core-diameter-mismatched fiber section," *IEEE Photon. J.*, vol. 2, no. 2, pp. 152–157, Apr. 2010.

[17] W. Qian, G. Farrell, and W. Yan, "Investigation on single-mode–multimode–single-mode fiber structure," *J. Lightw. Technol.*, vol. 26, no. 5–8, pp. 512–519, Mar./Apr. 2008.

[18] C.-L. Zhao, X. F. Yang, M. S. Demokan, and W. Jin, "Simultaneous temperature and refractive index measurement using a 3 degrees slanted multimode fiber Bragg grating," *J. Lightw. Technol.*, vol. 24, no. 2, pp. 879–883, Feb. 2006.

[19] O. Frazão, J. Viegas, P. Caldas, J. L. Santos, F. M. Araújo, L. A. Ferreira, and F. Farahi, "All-fiber Mach–Zehnder curvature sensor based on multimode interference combined with a long-period grating," *Opt. Lett.*, vol. 32, no. 21, pp. 3074–3076, Nov. 2007.